CRYSTAL GROWTH & DESIGN

pubs.acs.org/crystal

Communication

Photoreactive Polymorphic Cocrystals Utilizing a Molecular Template with Dual Halogen and Hydrogen Bonding Capabilities

Published as part of the Crystal Growth & Design virtual special issue "Lattice Dynamics".

Eric Bosch,* Conrad J. Powell, Herman R. Krueger, Jr., and Ryan H. Groeneman*

Cite This: *Cryst. Growth Des.* 2023, 23, 3947−3951

Read Online

ACCESS | Metrics & More | Article Recommendations | Supporting Information

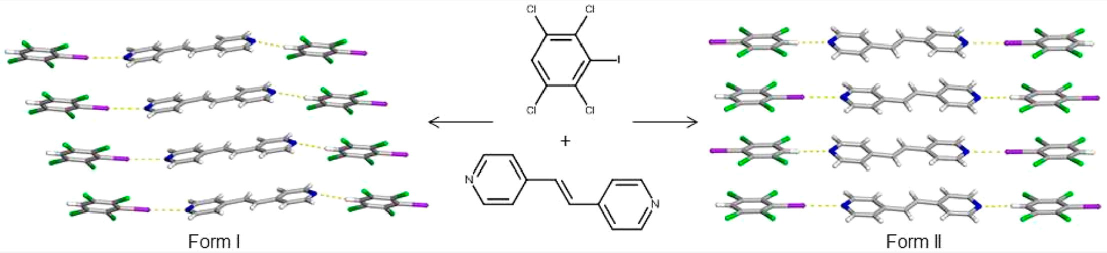

ABSTRACT: The ability of 1,2,4,5-tetrachloro-3-iodobenzene to act as a template to form a pair of polymorphic cocrystals with *trans*-1,2-bis(4-pyridyl)ethylene is reported. After exposure to ultraviolet light, a nearly quantitative yield for the [2 + 2] cycloaddition reaction was observed for both concomitant cocrystals. These crystalline solids engage in both I···N halogen bonds along with nontraditional C−H···N hydrogen bond which results in a one-dimensional chain. In addition, the components homogeneous $\pi-\pi$ stack which positions the carbon−carbon double bond on the reactant molecule in a suitable orientation to undergo a photoinduced cyclization reaction.

■ INTRODUCTION

The intentional design of molecular cocrystals with predictable and controllable properties remains a central goal for crystal engineers and materials scientists.[1] A cocrystal is defined as a crystalline solid that contains at least two different molecules in a fixed whole-number ratio. A successful approach in the formation of these cocrystals is to utilize complementary halogen- and/or hydrogen-bonding interactions in order for these molecules to recognize each other and then self-assemble into a multicomponent solid.[2]

A current area of research, within our groups, is the formation of halogen-bonded cocrystals that will undergo the solid-state [2 + 2] cycloaddition reaction.[3−5] In particular, we have focused on utilizing I···N halogen bonds from chlorine-substituted iodobenzenes, since these halogen-bond donors tend to $\pi-\pi$ stack in an infinite and homogeneous pattern.[6] As a result of this noncovalent interaction, various pyridine-based reactant molecules will also engage in this homogeneous stacking which ultimately places a pair of carbon−carbon double bonds (C═C) in a suitable position to photoreact. Initially, we reported the ability of 1,4-diiodoperchlorobenzene ($C_6I_2Cl_4$) to template a photoreaction by engaging in I···N halogen bonds along with homogeneous $\pi-\pi$-stack interactions with *trans*-1,2-bis(4-pyridyl)ethylene (BPE).[7] The reliability of this chlorine-based halogen-bond donor to form these homogeneous π-stacks is key in the formation of a photoreactive cocrystal. In contrast, the stronger halogen-bond donor, 1,4-diiodotetrafluorobenzene also forms cocrystals with BPE where the two components alternately π-stack resulting in a photostable solid.[8] In related research, the ability of both 1,2,4,5-tetrabromobenzene and 1,2,4,5-tetrachlorobenzene to form nontraditional C−H···N hydrogen bonds along with this homogeneous $\pi-\pi$ stacking also resulted in photoreactive cocrystals with BPE.[9,10]

Utilizing the tendencies for chlorinated benzenes to stack in an infinite array,[6] it was envisioned that by changing one of the iodine atoms on $C_6I_2Cl_4$ to a hydrogen resulting in 1,2,4,5-tetrachloro-3-iodobenzene (C_6HICl_4) (Scheme 1a) would allow this molecule to engage in both halogen- and hydrogen-bonding interactions with BPE. In addition, C_6HICl_4 was also expected to engage in an infinite face-to-face π-stacking arrangement observed in other chlorine-substituted iodobenzenes thereby facilitating a similar π-stacking pattern for BPE.

Using this as inspiration, we report here the ability of C_6HICl_4 to act as both a halogen- and hydrogen-bond donor

Received: March 9, 2023
Revised: April 26, 2023
Published: May 9, 2023

https://doi.org/10.1021/acs.cgd.3c00304
Cryst. Growth Des. 2023, 23, 3947−3951

Scheme 1. Renderings of (a) the Template 1,2,4,5-Tetrachloro-3-iodobenzene C_6HICl_4 and (b) the Solid-State [2 + 2] Cycloaddition Reaction

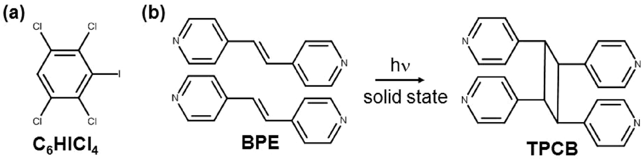

to form a pair of photoreactive polymorphic cocrystals with the formula $(C_6HICl_4)\cdot(BPE)$. In particular, both polymorphs undergo a nearly quantitative [2 + 2] cycloaddition reaction generating *rctt*-tetrakis(4-pyridyl)cyclobutane (TPCB) in the organic solid state (Scheme 1b). To the best of our knowledge, this is the first molecular template that forms concomitant halogen and hydrogen bonds to generate a photoreactive solid. Similar cooperative halogen and hydrogen bonding has been reported in cocrystals containing BPE along with 1,2,4,5-tetrafluoro-3-iodobenzene and 1-bromo-2,3,4,5-tetrafluorobenzene although these halobenzenes do not π-stack in a homogeneous pattern in these cocrystals.[11] Consequently, neighboring C═C are well beyond the accepted distance for a photoreaction.[12]

To evaluate the halogen- and hydrogen-bonding propensity of C_6HICl_4 a molecular electrostatic potential calculation was performed. This surface calculation returned two large positive σ-holes that were found on the iodine atom (136.3 kJ/mol) and the hydrogen atom with a nearly identical value (135.9 kJ/mol) supporting our expectation that these donor atoms are capable of forming concomitant halogen and hydrogen bonding interactions (Figure 1). In contrast, the chlorine atoms have a drastically lower positive charge with values of 78.1 and 76.3 kJ/mol for the *meta*- and *ortho*-position with respect to the iodine, respectively. As a result, these chlorine atoms are not expected to participate in halogen-bonding interactions rather forming secondary chlorine−chlorine contacts within single- and multicomponent solids.

The template C_6HICl_4 was synthesized from 2,3,5,6-tetrachloroaniline by sequential diazotization-iodination as previously reported for the synthesis of 1,3,5-trichloro-2-iodobenzene.[13] This dual donor molecule was previously synthesized by iodination of the Grignard reagent prepared from pentachlorobenzene.[14] Single-crystals of C_6HICl_4 suitable for X-ray diffraction were realized by slow evaporation of a solution containing 0.3 g within 6 mL of 1:1 hexane and ethyl acetate.

X-ray diffraction data revealed that C_6HICl_4 crystallizes in the centrosymmetric orthorhombic space group $Pbc2_1$ that contains a single molecule in the asymmetric unit. As seen with other chlorinated iodobenzenes, molecules of C_6HICl_4 π-stack in an infinite and face-to-face arrangement where the iodine are located in a *syn* orientation within each column (Figure 2).

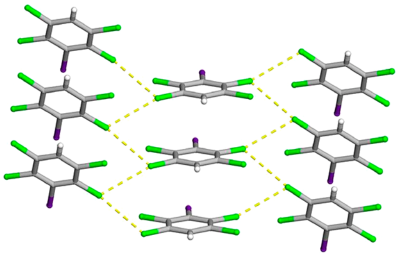

Figure 2. X-ray structure of C_6HICl_4 illustrating the infinite face-to-face π−π stacking of the aromatic rings along with chlorine-chlorine contacts. Cl···Cl contacts shown as yellow dashed lines.

The centroid-centroid distance between neighboring aromatic rings is 4.0143(3) Å which is equal to the crystallographic *b*-axis. These stacked rings interact with nearest columns via chlorine-chlorine contacts [Cl···Cl 3.511(3), 3.521(3) Å; C−Cl···Cl 148.7(3), 148.5(3)°] that are similar to trifurcated X_3 synthon observed in other perhalobenzenes (Figure 2).[6,15,16] Lastly, these donors also interact via Type II I···Cl interactions[17] [I···Cl 3.5608(16) Å; C−I···Cl 162.52(15)°; C−Cl···I 94.4(2)°] that results in a wave-like one-dimensional chain that lies along the crystallographic *c*-axis (Figure 3).

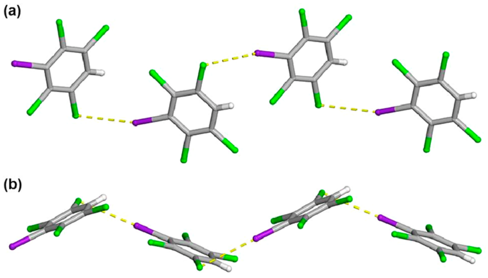

Figure 3. X-ray structure of C_6HICl_4 illustrating the (a) Type II I···Cl interactions and (b) the wave-like pattern for the one-dimensional chain. Type II I···Cl interactions shown as yellow dashed lines.

The formation of a pair of polymorphic cocrystals containing C_6HICl_4 as a dual halogen- and hydrogen-bond donor was achieved. Both polymorphs were present regardless of the evaporation rate of the solvent. These polymorphs were realized by taking a 1:1 molar ratio of C_6HICl_4 and BPE in toluene which was then allowed to evaporate. The evaporation rate was controlled by the position of the cap on the scintillation vial. In particular, the faster evaporation occurred when the cap was completely removed while the slower approach took place when the cap was turned upside down

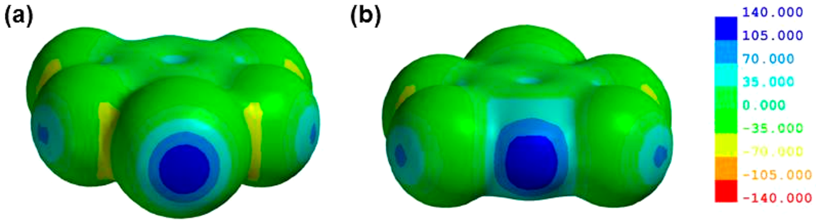

Figure 1. Molecular electrostatic potential plot of C_6HICl_4 illustrating the σ-hole on the (a) iodine and (b) hydrogen atom. The units for the scale are in kJ/mol.

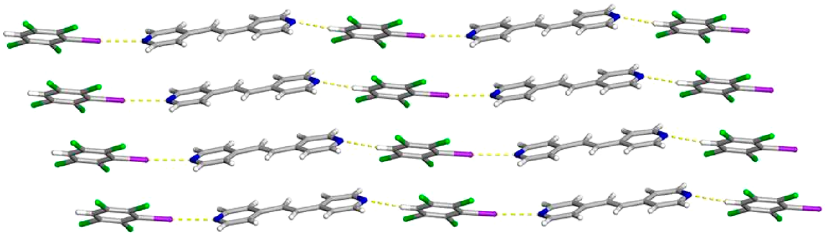

Figure 4. X-ray structure of Form I of $(C_6HICl_4)\cdot(BPE)$ illustrating both the halogen- and hydrogen-bonding interactions that result in an one-dimensional chain along with the *syn*-orientation of the iodine atoms on neighboring donors. I···N halogen bonds and the C−H···N hydrogen bonds shown as yellow dashed lines.

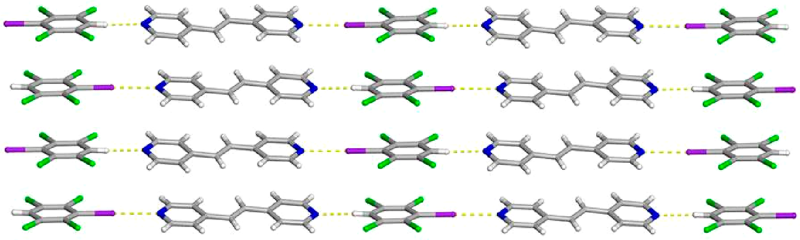

Figure 5. X-ray structure of Form II of $(C_6HICl_4)\cdot(BPE)$ illustrating both the halogen- and hydrogen-bonding interactions that result in an one-dimensional chain along with the *anti*-orientation of the iodine atoms on neighboring donors. The I···N halogen bonds and the C−H···N hydrogen bonds shown as yellow dashed lines.

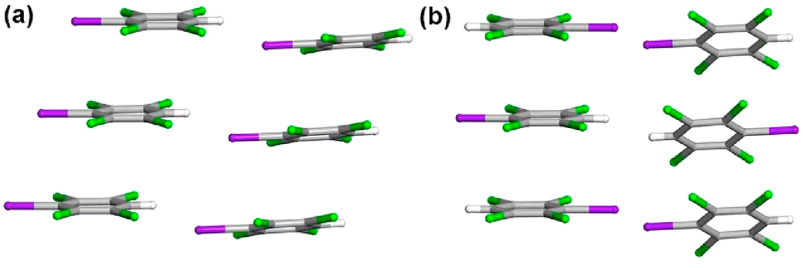

Figure 6. View of both independent molecules of C_6HICl_4 within (a) Form I and (b) Form II highlighting the different offset π-stacking in both polymorphs.

and placed off center to the vial's opening. Both approaches afforded single crystals suitable for X-ray diffraction for each polymorph.

Crystallographic analysis revealed that both polymorphs had a formula of $(C_6HICl_4)\cdot(BPE)$. Form I crystallizes in the centrosymmetric monoclinic space group $P2_1/n$. Within the asymmetric unit of Form I are two molecules of C_6HICl_4 and BPE. These crystallographically unique pairs are found to engage in both I···N halogen bonds [I···N 2.833(3), 2.896(4) Å; C−I···N 179.17(12), 173.99(12)°] along with a C−H···N hydrogen bond [C···N 3.292(5), 3.399(5) Å; C−H···N 158.6(4), 173.0(4)°] to produce a pair of one-dimensional chains (Figure 4). The ethylene bridges within both BPE molecules are found to be ordered at room temperature. Within a given polymer chain, the aromatic rings on C_6HICl_4 and the interacting pyridyl ring of BPE are found at varying angles, namely a set is nearly coplanar with interplanar angles of 5.99(2) and 7.729(2)° while the other is twisted with interplanar angles of 33.10(17) and 32.70(15)°. Importantly, both unique C_6HICl_4 molecules are found to engage in a face-to-face offset $\pi-\pi$ stacking arrangement that yields an infinite column where the iodine atoms are *syn* to its nearest neighboring donor (Figure 4). As a result of this homogeneous $\pi-\pi$ stacking arrangement of the donors, both unique BPE molecules are also found in an infinite stack generating a C═C distance of 4.0505(1) which is equal to the crystallographic *a*-axis and within the accepted limit of 4.2 Å for a photoreaction.[12]

Unlike Form I, single-crystal X-ray diffraction data revealed that Form II crystallizes in the centrosymmetric triclinic space group $P\overline{1}$. Again, the asymmetric unit has two molecules of both C_6HICl_4 and BPE within Form II. These donor and acceptor pairs are also found to engage in both I···N halogen bonds [I···N 2.832(7), 2.818(7) Å; C−I···N 177.7(2), 178.2(2)°] along with a C−H···N hydrogen bond [C···N 3.216(12), 3.323(12) Å; C−H···N 178.3(7), 178.2(9)°] to generate two crystallographically unique one-dimensional chains (Figure 5). Again, both ethylene bridges within BPE are ordered at room temperature. Within Form II, the torsional angles between C_6HICl_4 and the interacting pyridyl ring of BPE are closer to coplanar with interplanar angles of 8.3(3), 10.4(3), 7.6(3), and 5.7(3)°. These donor and acceptor molecules are again found to stack in a homogeneous face-to-face arrangement which yields an infinite column; however, in Form II the iodine atoms are now *anti* to its nearest neighbor (Figures 5 and 6). It is noteworthy that the alternating orientation of the iodine atoms facilitates slightly closer π-stacking with more face-to-face contact and two unique interplanar plane-to-centroid distances of 3.622(8) and 3.647(7) Å, respectively. In contrast, within Form I molecules of C_6HICl_4 are uniformly offset slip-stacked with a plane-centroid distance of 3.687(3) Å. Within Form II, there are four unique C═C distances ranging from 3.812 to 4.061 Å measured from the centroids between the ethylene carbons. As with Form I, all of these distances are well within the limit for a [2 + 2] cycloaddition reaction.[12]

The bulk material from both evaporation rates were investigated by powder X-ray diffraction to determine the relative amounts of each polymorph present in the resulting solid. The two cocrystal samples (*i.e.* fast and slow evaporation) were allowed to dry to completeness and ground to a powder using a mortar and pestle. Then the particular solid was transferred to a powder diffractometer for data collection (Figures S1 and S2). The resulting diffractograms were compared to the calculated single-crystal structure for each polymorph to determine the relative amount of each cocrystal in the bulk phase. In particular, the resulting whole pattern fitting algorithm calculation for the fast evaporation vial returned values of 65% for Form I and 35% for Form II (Figure S3). While the slower evaporation vial had values of 79% and 21% for Form I and Form II, respectively (Figure S4).

In order to determine if a [2 + 2] cycloaddition reaction would occur for either solid a powdered sample of each mixture of polymorphs were placed between glass plates and placed in a photoreactor. Both samples were exposed to broadband UV radiation from a 450 W medium-pressure mercury vapor bulb. A photoreaction was detected in both the fast and the slow evaporation rate solids as confirmed by ^1H NMR spectroscopy. In particular, the olefin peak for BPE located at 7.55 ppm decreased (Figure S5) with concomitant appearance of the cyclobutane peak of TPCB at 4.67 ppm (Figures S6 and S7) confirming the occurrence of a photoreaction.[18] After 30 h of irradiation, integration of the two peaks indicated an overall yield of 96% for the [2 + 2] cycloaddition reaction for each polymorph containing solid. It is noteworthy that a similar yield was observed for a cocrystal containing iodoperchlorobenzene with BPE.[19]

To gain insight into the binding energies within these two polymorphs a Density Functional Theory (DFT) calculation was performed using the Gaussian 16 package. In particular, the M06-2X functional was used along with the aug-cc-pVTZ basis set for all DFT calculations. The halogen- and hydrogen-bonding energies were determined along with the homogeneous $\pi-\pi$ stacking between neighboring $C_6I_2Cl_4$ molecules for each polymorph. These energies were calculated by using atomic positions based upon X-ray diffraction data. In the case of hydrogen atoms, the positions were refined by performing a molecular mechanics optimization in which the positions of all other elements were frozen at the diffraction determined values. The I···N halogen-bonding complexation energies were similar with values of −23.5 and −22.7 kJ/mol for Form I and Form II, respectively. In terms of the C−H···N hydrogen bonds, the DFT calculations returned values of −12.0 kJ/mol for Form I and −15.3 kJ/mol for Form II. Lastly, the greatest energy difference was observed on comparing the homogeneous stacking of C_6HICl_4 within each polymorph. In particular, the *syn*-orientation within Form I had a smaller complexation energy, namely −29.7 kJ/mol, while that for the *anti-* orientation in Form II was significantly higher at −39.4 kJ/mol. The greater $\pi-\pi$ stacking energy for the *anti*-configuration is reasonable, since the larger iodine atoms do not have any steric interaction permitting slightly closer π-stacking with more extensive overlap.

■ CONCLUSION

In this contribution, we report the formation and photoreactivity of a pair of polymorphs with a formula of $(C_6HICl_4)\cdot(BPE)$. Powder X-ray diffraction confirmed that both polymorphs were obtained as a mixture irrespective of the evaporation rate of the solvent. In each mixed solid, the polymorphs underwent a [2 + 2] cycloaddition reaction with identical yields of 96%. Currently, we are expanding this research into unsymmetrical reactant molecules along with studying stoichiometric polymorphs of these original components.

■ ASSOCIATED CONTENT

Supporting Information

The Supporting Information is available free of charge at https://pubs.acs.org/doi/10.1021/acs.cgd.3c00304.

> Experimental details, X-ray crystallographic data, computational chemistry details, ^1H NMR spectra, and powder diffractograms (PDF)

Accession Codes

CCDC 2246379−2246381 contain the supplementary crystallographic data for this paper. These data can be obtained free of charge via www.ccdc.cam.ac.uk/data_request/cif, or by emailing data_request@ccdc.cam.ac.uk, or by contacting The Cambridge Crystallographic Data Centre, 12 Union Road, Cambridge CB2 1EZ, UK; fax: +44 1223 336033.

■ AUTHOR INFORMATION

Corresponding Authors

Eric Bosch − *Department of Chemistry and Biochemistry, Missouri State University, Springfield, Missouri 65897, United States;* orcid.org/0000-0002-6465-1879; Phone: +1 417-836-4277; Email: ericbosch@missouristate.edu

Ryan H. Groeneman − *Department of Biological Sciences, Webster University, St. Louis, Missouri 63119, United States;* orcid.org/0000-0002-4602-6287; Phone: +1 314-246-7466; Email: ryangroeneman19@webster.edu

Authors

Conrad J. Powell − *Department of Biological Sciences, Webster University, St. Louis, Missouri 63119, United States*

Herman R. Krueger, Jr. − *Department of Biological Sciences, Webster University, St. Louis, Missouri 63119, United States*

Complete contact information is available at: https://pubs.acs.org/10.1021/acs.cgd.3c00304

Author Contributions

The manuscript was written through contributions of all authors. All authors have given approval to the final version of the manuscript.

Notes

The authors declare no competing financial interest.

■ ACKNOWLEDGMENTS

R.H.G. gratefully acknowledges financial support from Webster University in the form of various Faculty Research Grants. E.B. acknowledges The National Science Foundation, Division of Chemistry, Major Research Instrumentation Program that funded the purchase of the Synergy-S X-ray diffractometer, Award Number 2117129. Dr. Daniel Unruh from the

University of Iowa is also acknowledged for collecting the powder X-ray diffraction patterns.

■ REFERENCES

(1) Aakeröy, C. B.; Salmon, D. B. Building co-crystals with molecular sense and supramolecular sensibility. *CrystEngComm* **2005**, *7*, 439−448.

(2) Corpinot, M. K.; Bučar, D.-K. A Practical Guide to the Design of Molecular Crystals. *Cryst. Growth Des.* **2019**, *19*, 1426−1453.

(3) Bosch, E.; Kruse, S. J.; Reinheimer, E. W.; Rath, N. P.; Groeneman, R. H. Regioselective [2 + 2] cycloaddition reaction within a pair of polymorphic co-crystals based upon halogen bonding interactions. *CrystEngComm* **2019**, *21*, 6671−6675.

(4) Kruse, S. J.; Bosch, E.; Brown, F.; Groeneman, R. H. Incorporating Ester Functionality within a Solid-State [2 + 2] Cycloaddition Reaction Based Upon Halogen Bonding Interactions. *Cryst. Growth Des.* **2020**, *20*, 1969−1974.

(5) Bosch, E.; Battle, J. D.; Groeneman, R. H. Crystal structure and photoreactivity of a halogen-bonded cocrystal based upon 1,2-diiodoperchlorobenzene and 1,2-bis(pyridin-4-yl)ethylene. *Acta Crystallogr.* **2020**, *C76*, 557−561.

(6) Reddy, C. M.; Kirchner, M. T.; Gundakaram, R. C.; Padmanabhan, K. A.; Desiraju, G. R. Isostructurality, Polymorphism and Mechanical Properties of Some Hexahalogenated Benzenes: The Nature of Halogen···Halogen Interactions. *Chem.—Eur. J.* **2006**, *12*, 2222−2234.

(7) Bosch, E.; Kruse, S. J.; Krueger, H. R.; Groeneman, R. H. Role of $\pi-\pi$ Stacking and Halogen Bonding by 1,4-Diiodoperchlorobenzene To Organize the Solid State To Achieve a [2 + 2] Cycloaddition Reaction. *Cryst. Growth Des.* **2019**, *19*, 3092−3096.

(8) Walsh, R. B.; Padgett, C. W.; Metrangolo, P.; Resnati, G.; Hanks, T. W.; Pennington, W. T. Crystal Engineering through Halogen Bonding: Complexes of Nitrogen Heterocycles with Organic Iodides. *Cryst. Growth Des.* **2001**, *1*, 165−175.

(9) Santana, C. M.; Reinheimer, E. W.; Krueger, H. R.; MacGillivray, L. R.; Groeneman, R. H. Edge-to-Edge C−H···N Hydrogen Bonds in Two-Component Co-crystals Aide a [2 + 2] Photodimerization. *Cryst. Growth Des.* **2017**, *17*, 2054−2058.

(10) Grobelny, A. L.; Verdu, F. A.; Groeneman, R. H. Solvent-free synthesis and purification of a photoproduct *via* sublimation of a tetrahalogenated template. *CrystEngComm* **2017**, *19*, 3562−3565.

(11) Bosch, E.; Bowling, N. P. Supramolecular Polymer Formation Featuring Cooperative Halogen Bonding and Nonconventional sp^2-CH···N Hydrogen Bonding. *Cryst. Growth Des.* **2019**, *19*, 5929−5933.

(12) Schmidt, G. M. J. Photodimerization in the solid state. *Pure Appl. Chem.* **1971**, *27*, 647−678.

(13) Krasnokutskaya, E. A.; Semenischeva, N. I.; Filimonov, V. D.; Knochel, P. A New, One-Step, Effective Protocol for the Iodination of Aromatic and Heterocyclic Compounds via Aprotic Diazotization of Amines. *Synthesis* **2007**, 81−84.

(14) Rahman, M. T. The preparation and some reactions of 2, 3, 5, 6-tetrachlorophenylmagnesium chloride. *J. Organomet. Chem.* **1982**, *225*, 25−30.

(15) Bosch, E.; Barnes, C. L. Triangular Halogen−Halogen−Halogen Interactions as a Cohesive Force in the Structures of Trihalomesitylenes. *Cryst. Growth Des.* **2002**, *2*, 299−302.

(16) Krueger, H. R.; Shapiro, N. M.; Bosch, E.; Unruh, D. K.; Groeneman, R. H. Influence of Secondary Interactions on Structural Diversity between a Pair of Halogen-Bonded Co-Crystals Containing Isosteric Donors. *Compounds* **2022**, *2*, 285.

(17) Mukherjee, A.; Tothadi, S.; Desiraju, G. R. Halogen Bonds in Crystal Engineering: Like Hydrogen Bonds yet Different. *Acc. Chem. Res.* **2014**, *47*, 2514−2524.

(18) MacGillivray, L. R.; Reid, J. L.; Ripmeester, J. A. Supramolecular Control of Reactivity in the Solid State Using Linear Molecular Templates. *J. Am. Chem. Soc.* **2000**, *122*, 7817−7818.

(19) Shapiro, N. M.; Bosch, E.; Unruh, D. K.; Krueger, H. R.; Groeneman, R. H. Iodoperchlorobenzene acts as a dual halogen-bond donor to template a [2 + 2] cycloaddition reaction within an organic co-crystal. *CrystEngComm* **2021**, *23*, 8265−8268.

https://doi.org/10.1021/acs.cgd.3c00304
Cryst. Growth Des. 2023, 23, 3947−3951